AD_____

Award Number: W81XWH-12-1-0188

TITLE: The Role of CHD1 in DNA Rearrangements and Progression of Prostate Cancer

PRINCIPAL INVESTIGATOR: Wennuan Liu, Ph.D.
Siqun Lilly Zheng, M.D.
Jielin Sun
Junjie Feng
Tao Li

CONTRACTING ORGANIZATION:
Wake Forest University Health Sciences
Winston Salem, NC 27157

REPORT DATE: July 2013

TYPE OF REPORT: Annual

PREPARED FOR: U.S. Army Medical Research and Materiel Command
Fort Detrick, Maryland 21702-5012

DISTRIBUTION STATEMENT: (

■ Approved for public release; distribution unlimited

REPORT DOCUMENTATION PAGE

Form Approved
OMB No. 0704-0188

1. REPORT DATE *(DD-MM-YYYY)*	**2. REPORT TYPE**	**3. DATES COVERED** *(From - To)*
07-31-2013	Annual	01 July 2012 – 30 June 2013

4. TITLE AND SUBTITLE
The Role of CHD1 in DNA Rearrangements and Progression of Prostate Cancer

a. CONTRACT NUMBER

5b. GRANT NUMBER
W81XWH-12-1-0188

5c. PROGRAM ELEMENT NUMBER

6. AUTHOR(S)
Wennuan Liu, Siqun Zheng, Jielin Sun,
Junjie Feng

weliu@wakehealth.edu

5d. PROJECT NUMBER

5e. TASK NUMBER

5f. WORK UNIT NUMBER

7. PERFORMING ORGANIZATION NAME(S) AND ADDRESS(ES)
Wake Forest University Health Sciences
Medical Center Boulevard
Winston Salem, NC 27157

8. PERFORMING ORGANIZATION REPORT NUMBER

9. SPONSORING / MONITORING AGENCY NAME(S) AND ADDRESS(ES)
U.S. Army Medical Research and Materiel Command
Fort Detrick, Maryland 21702-5012

10. SPONSOR/MONITOR'S ACRONYM(S)

11. SPONSOR/MONITOR'S REPORT NUMBER(S)

12. DISTRIBUTION / AVAILABILITY STATEMENT
Approved for public release; distribution unlimited

13. SUPPLEMENTARY NOTES

14. ABSTRACT

Most prostate cancers (PCa) are considered to be indolent (non-aggressive) and may not even require treatment. However, some of them are aggressive tumors that are characterized by DNA rearrangements resulting in cancer progression, recurrence and metastases, leading to ~ 30,000 deaths in the U.S. annually. We hypothesize that the chromatin remodeler encoded by *CHD1* affects the genesis and/or location of DNA rearrangement breakpoints which cause DNA copy number alterations (CNAs) at a number of genes, thereby playing a role in the development and progression of PCa. Specifically, we postulate that 1) loss of the *CHD1* gene is associated with DNA rearrangements at particular locations in the tumor genome of PCa; 2) experimental knockout of Chd1 protein expression will lead to specific DNA copy number changes at genes that are concurrently altered with the *CHD1* gene in PCa tumors; and 3) down-regulation of *CHD1* expression and its collaborative gene(s), including *MAP3K7*, will result in tumorigenesis and invasion of tumor cells. Using DNA of tumor and matched normal cells from multiple patient cohorts, genome-wide SNP arrays and the algorithm of Genomic Identification of Significant Targets in Cancer (GISTIC), we have identified and validated that 1) *CHD1* is second only to *PTEN* as the most frequent homozygously deleted gene in PCa, and 2) tumors with loss of *CHD1* represent a unique and distinct subtype of PCa. We further demonstrated that 1) complete loss of *CHD1* is associated with a larger number of homozygous deletions (HODs) at other locations in the tumor genome, and 2) loss of *CHD1* is associated with deletions on 2q22, 5q11.2 and 6q15 in the tumor genome. Together with the deletions observed in HEK293 cells stably transfected with *CHD1* shRNA and dramatic morphological changes caused by down-regulation of Chd1 in mouse prostate epithelial cells, these data suggest a causal relationship, which warrants further investigation the role *CHD1* in PCa progression.

15. SUBJECT TERMS
CHD1, MAP3K7, CNA's

16. SECURITY CLASSIFICATION OF:			**17. LIMITATION OF ABSTRACT**	**18. NUMBER OF PAGES**	**19a. NAME OF RESPONSIBLE PERSON USAMRMC**
a. REPORT	**b. ABSTRACT**	**c. THIS PAGE**			**19b. TELEPHONE NUMBER** *(include area code)*
U	U	U	UU	18	

Table of Contents

INTRODUCTION

Most prostate cancers (PCa) are considered to be indolent (non-aggressive) and may not even require treatment. However, some of them are aggressive tumors that are characterized by uncontrolled cell proliferation resulting in cancer progression, recurrence and metastases, leading to ~ 30,000 deaths in the U.S. annually. Our inability to reliably distinguish between these two forms of the disease, especially at early stages, has resulted in over-treatment of many and under treatment of some. Therefore, it is critical to identify markers that can distinguish these two types of PCa patients at the time of diagnosis, as well as genes that drive cancer progression. Since the utility of clinicopathologic parameters in distinguishing lethal from indolent forms of prostate cancer PCa is very limited, especially at an early stage, considerable effort has been made to identify molecular markers that can be used to identify lethal PCa and predict disease outcomes. However, few of them are able to reliably distinguish lethal PCa from indolent forms. PCa is a genetic disease whose tumor genome is characterized by diverse somatic mutations and pathway alterations derived from complex DNA rearrangements. In the tumor genome, the most common alterations are primarily composed of gains, losses, and rearrangements of genomic DNA. Thus, analysis of copy number alterations or abnormalities (CNAs) in tumor genomes provides insights into the specific genes and molecular pathways that promote tumorigenesis and determine the clinical course. In our pilot study, our preliminary data revealed that: 1) *CHD1* is second only to *PTEN* as the most frequent homozygously deleted gene in the tumor genome of PCa; 2) complete loss of *CHD1* is associated with a larger number of homozygous deletions (HODs) at other locations in the tumor genome; and 3) loss of *CHD1* is associated with deletions on 2q22, 5q11.2 and 6q15 in the tumor genome. Therefore, our overall hypothesis is that *CHD1* affects the genesis and/or location of DNA rearrangement breakpoints that which in CNAs at a number of genes, thereby playing a role in the development and progression of PCa.

In this DOD supported research, we proposed: **1)** To assess the correlations between *CHD1* associated CNAs/genes and clinicopathologic characteristics in PCa using clinical specimens and genome wide analysis of DNA; **2)** To evaluate the *in vitro* effects of knockdown expression of *CHD1* on response to oxidative stress, genesis of DNA rearrangement in term of CNAs, deferentially altered gene expression profile, and cellular and growth characteristics; and **3)** To explore the *in vivo* joint effects of *CHD1* and the collaborative gene *MAP3K7* on tumorigenesis, cell proliferation (Ki67), tumor size, histopathological characteristics, invasion and metastases, using tissue recombination with UGM and PrP/SC grafted under the renal capsule and subcutaneous xenografts in nude mice.

BODY

Approved Statement of Work:

Objective/Aim 1): To assess the correlations between *CHD1* associated CNAs/genes and clinicopathologic characteristics in PCa. Dr. Liu's team at Wake Forest University Health Sciences will be responsible for this aim.

Task 1). Update clinical information of study subjects and isolates genomic DNA
- Months 1- 10

Task 2). 6.0 SNP array assay, confirmation and DNA copy number analysis
- Months 10-12

Task 3). Obtain clinical information and perform association analysis
- Months 6-12

Objective /Aim 2): To evaluate the *in vitro* effects of knockdown expression of *CHD1*. Dr. Liu's team at Wake Forest University Health Sciences will be responsible for this aim.

Task 1). Develop cell lines with knockdown expression of *CHD1* and Tak1 (MAP3K7) -Months 1-12

Task 2). Biological characterization of cell lines with knockdown of Chd1 -Months 10-13

Task 3). Evaluate the protective role of *CHD1* via Comet assay -Months 12-15

Task 4). Develop clonal cell lines from cells treated with H_2O_2 -Months 14-17

Task 5). Analyze CNAs in cell lines with knockdown *CHD*1/treated with H_2O_2 -Months 17-22

Task 6). Analyze transcriptome in cell lines with knockdown *CHD1* -Months 17-22

Task 7). Scientific communication of results - Months 12-36

.

Objective/Aim 3): To explore the *in vivo* joint effects of *CHD1* and the collaborative gene (MAP3K7). Dr. Cramer's team at UCD will be responsible for this aim. Dr. Liu's team will be responsible for analysis of CNAs in xenografts.

Task 1). Characterization of cells with double-knockdown of *CHD1* and Tak1 -Months 10-13

Task 2). Characterization of WFU3 cells with Chd1 and Tak1 (*MAP3K7*) knockdown cells -Months 13-27

Task 3). Characterization of In Vivo phenotype of PC-3 cells with *CHD1* and Tak1 (*MAP3K7*) knockdown -Months 13, 24-30

Task 4). Analysis of CNAs in xenograft tumors -Months 30-33

Task 5). Scientific communication of results -Months 34-36

Overall scientific communication of results from all 3 objectives/aims - Months24-36

Summary report

We were in the 12th month of this funded project by July 2013. Here is a outline of the research that we have completed to date: 1) selected PCa cohorts and updated clinical data, 2) performed genome-wide DNA copy number analysis and assessed the associations between *CHD1* associated CNAs/genes and clinicopathologic characteristics in PCa, 3) generated a number of cell lines with knockdown levels of *CHD1*/*MAP3K7* and performed initial evaluation and exploratory analysis of cell lines with knockdown of Chd1expression.

Detailed report

Study Design: Since our grant proposal was submitted, raw data from additional PCa cohorts generated by us have become available. Therefore, in addition to original PCa cohort, we also include other cohorts in our current study design in order to comprehensively assess the

correlations between *CHD1* associated CNAs/genes and clinicopathologic characteristics in PCa for Aim 1.

Study subjects and DNA copy number analysis: Somatic tumor DNA from a total of 22 xenografts of PCa, 91 tumor metastases of 30 autopsy patients and 244 PCa patients undergoing radical prostatectomy (RP) for treatment of clinically localized disease at two centers, one in the US, [Johns Hopkins Hospital (JHH)] and the other in Sweden [Karolinska Institute (KI)] from 1988 to 2006 was used in this study. They were selected based on the availability of genomic DNA of sufficient quantity (>5μg) and purity (>70% cancer cells for cancer specimens, no detectable cancer cells for normal samples). Tissue samples were obtained by macro-dissection of matched non-malignant (normal) and cancer containing areas of prostate tissue as determined by histological evaluation of H&E stained frozen sections of snap frozen RP specimens. Amongst these 244 patients, 193 had normal control DNA, while 51 of them had no matched normal DNA available at the time of DNA analysis.

Most of the 141 patients in the JHH cohort had a more aggressive form of PCa; 31%, 30%, and 46% of patients, respectively had pathologic Gleason score ≥ 8, pathologic stage ≥ T3b, and pretreatment serum PSA ≥ 10 ng/mL. Some of the preliminary results from this JHH cohort were included in our original grant proposal, which will not be presented in this report.

Most of the 103 patients in the Swedish cohort had a less aggressive form of PCa; ~51% and ~ 11% of these patients had a pre-operative Gleason score ≤ 6 and a pathological Gleason score ≥ 8, respectively. Assay of SNP array, DNA copy number analysis and identification of target genes were carried out according to manufacturer's instructions.

RNAi and Western blot: The *CHD1* shRNAs were initially purchased from OriGene (Rockville, MD) and used for transfection of human cell lines following the manufacturer's instructions. These shRNAs include TI355777 (ATG ATG GAG CTA AAG AAA TGT TGT AAC CA), TI355778 (CAC AAG GAG CTT GAG CCA TTT CTG TTA CG), TI355779 (AGT GTC AGA TGC TCC AGT TCA TAT CAC GG), and TI355780 (AAT GGA CAC AGT GAT GAA GAA AGT GTT AG). Additional shRNAs were designed and constructed according to a previously published method[1, 2] for lentiviral infection of the mouse prostate epithelial cells (MPECs). We directly subcloned a control shRNA with a scrambled sequence of "GGG CCA TGG CAC GTA CGG CAA G" and a *CHD1* shRNA with a target sequence of "GAA GAT GTG GAA TAT TAT AAT T" into a lentiviral vector pLU containing a puromycin-resistant gene as previously described[3], in addition to the shRNAs against *CHD1* and non-specific target from OriGene. The shRNA-containing lentiviruses were packaged following a standard protocol[4] and used to infect MPECs[5]. Two days post infection, 1.5 μg/ml of puromycin was added to select the transfected cells for at least 3 days and then used for downstream assays. We performed immunostaining and Western bloting according to a previous protocol[2] with modifications using a *CHD1* antibody (Bethyl Laboratories, Inc, Montgomery, TX).

Clonogenic assay: Clonogenic analysis was performed as described previously[6]. Briefly, cells infected by the lentivirus expressing the control shRNA and *CHD1*shRNA were individually plated at different densities (125, 250, 500, 1000 and 2000 per dish) in 6-cm cell culture dishes. After 7-10 days, the cells were fixed in 10% formalin and stained by 0.1% crystal violet. Photoshop software was used to quantify the pixels of the stained cells.

Three-dimensional (3D) culture of the mouse prostate epithelial cells: According to a previously published method of 3D culture[5], MPECs infected by the control shRNA and *CHD1* shRNA were individually trypsinized and resuspended in the collagen matrix at a density of 8×10^4 cells/ml. A 0.5 ml aliquot of this solution was dispensed into each well of a 24-well plate (4×10^4 cells/well). After the gel solidified at room temperature, 1.0 ml of culture medium was added to the top of the gel in each

well. The cells were maintained in the 3-D culture for 8-14 days in a cell culture incubator with media changes every other day. At the end of the incubation period, the branch structures for pseudoductal morphogenesis were imaged using digital photomicrography and the amount of outgrowth from spheroids over time was determined using Photoshop and digital photomicrography.

Statistical methods: The significance in the number of additional HODs in the tumor genomes with complete loss of *CHD1* in comparison to those in the tumor genomes either with *PTEN* HOD or without CNAs at *PTEN* and/or *CHD1* was assessed using Wilcoxon's two sample test. We used Fisher's exact test to test the associations 1) between loss of *CHD1* and other significant CNAs identified by the algorithm of GISTIC[7] across the whole genome, and 2) between *CHD1* associated CNAs/genes and clinicopathologic characteristics in PCa. We used the binomial proportion test to assess the significance in the distribution of additional HODs in the tumors that harbored complete loss of *CHD1*. All the statistical analyses were performed using SAS software version 9.2 (SAS Institute Inc., Cary, NC).

Results

CHD1 is identified and confirmed to be the second most frequent homozygously deleted gene in PCa. Recurrent somatic deletions in the tumor genome, especially HODs, have been informative targets in the search for tumor suppressor genes. To uncover the full spectrum of HODs in various types of PCa and to confirm our preliminary results in primary PCa tumors from JHH, we performed a comprehensive analysis of DNA CNAs in the tumor genomes of 103 primary PCa patients, 22

Table 1. Screening for homozygous deletions (HOD) in significant CNAs regions of deletion identified by Genomic Identification of Significant Targets in Cancer (GISTIC)*

Representative gene	JHH		Sweden		Combined	
and CNA-region (Cytoband)	#	%	#	%	#	%
PTEN(10q23.31)	18	12.77	16	15.53	34	13.93
CHD1(5q21.1)	10	7.09	11	10.68	21	8.61
BNIP3L(8p21.2)	3	2.13	2	1.94	5	2.05
LRP1B(2q22.1)	2	1.42	3	2.91	5	2.05
RB1(13q14.2)	3	2.13	1	0.97	4	1.64
USP10(16q24.1)	1	0.71	2	1.94	3	1.23
TMPRSS2-ERG(21q22)	3	2.13	0	0.00	3	1.23
HTR3A(11q23.2)	2	1.42	N/A	N/A	2	0.82
RYPB(3p13)	2	1.42	0	0.00	2	0.82
MAP3K7(6q15)	1	0.71	1	0.97	2	0.82
TP53(17p13.1)	0	0.00	1	0.97	1	0.41
CDKN1B(12p13.1)	1	0.71	0	0.00	1	0.41
SERPINB5(18q21.33-22.1)	0	0.00	0	0.00	0	0.00
PDE4D(5q11.2)	0	0.00	0	0.00	0	0.00
DISC1(1q42.2)	0	0.00	0	0.00	0	0.00

N/A, not tested due to in significant in GISTIC analysis.

* GISTIC was used to distinguish CNAs that likely drive cancer growth from numerous random CNAs that accumulate during cancer development.

xenografts and 91 tumor metastases using high resolution SNP arrays (Affymetrix, Santa Clara, CA). Genome-wide allele specific analysis revealed multiple occurrences of *CHD1* HOD in both of the cohorts from JHH and KI, with frequencies of 7.1% and 10.7%, respectively (Table 1 and, Figures 1-2**)**. In comparison, HOD frequency at *PTEN* was observed in ~ 13% and 16%, respectively, of the sample in these two cohorts. Thus, at this resolution, *CHD1* is second only to *PTEN* as the most frequent homozygously deleted gene in the tumor genome of PCa.

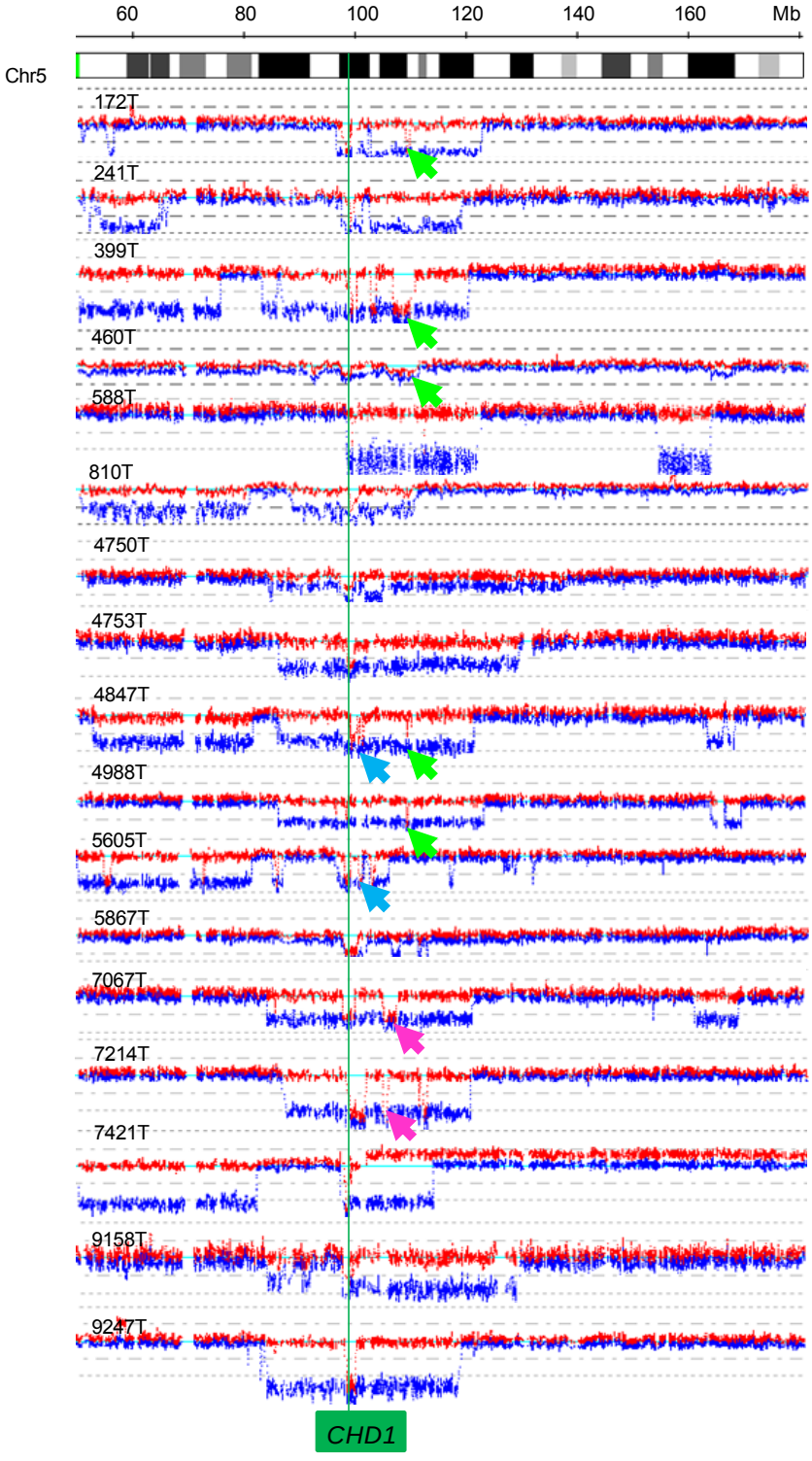

Figure 1. *CHD1* homozygous deletions on chromosomal region 5q revealed by allele specific analysis in PCa patients with radical prostatectomy. Blue and red dot-lines represent hybridization intensity of different alleles. Light-blue horizontal line is the baseline. Green vertical line depicts where *CHD1* is located. Same color arrows mark recurrent homozygous deletions in other regions of the genome. Tumor ID is labeled on the left

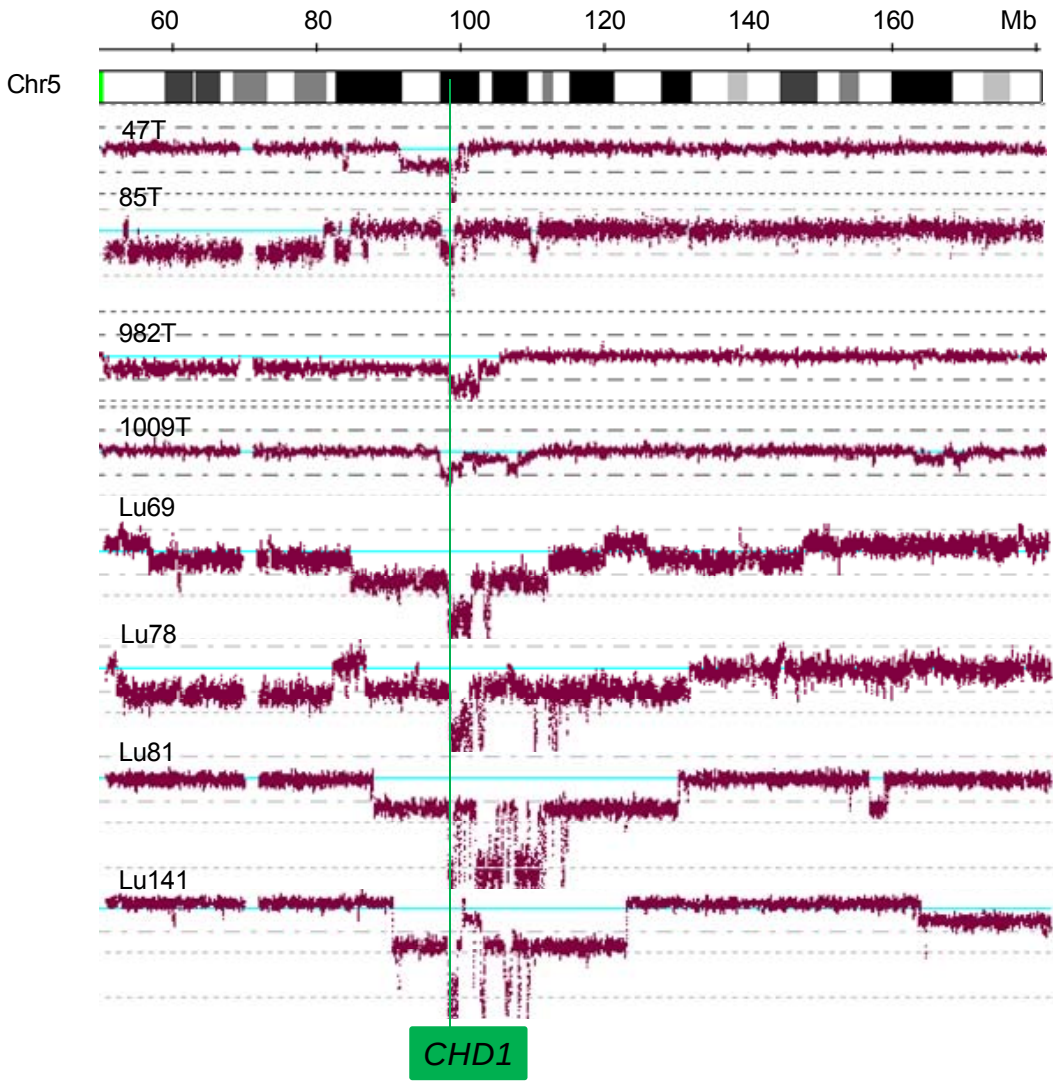

Figure 2. *CHD1* homozygous deletions on chromosomal region 5q revealed by non-allele specific analysis in PCa patients with radical prostatectomy. Green vertical line depicts where *CHD1* is located. Light blue horizontal line is the baseline. Brown horizontal dot-lines represent hybridization intensity data from non-allele specific analysis. Tumor ID is labeled on the left. Lu69, Lu78, Lu81 and Lu141 are PCa xenografts.

In primary PCa tumors, the size of HODs affecting *CHD1* ranged from ~138 kb to 2,898 kb, in some instances covering *RGMG*, *FAM174A* and *ST8SIA4*, in addition to *CHD1* (Table 2). Three of the HODs eliminated the 5' region of *CHD1*, while the majority removed the whole gene. Three of the HODs removed the 3' coding region of *CHD1*. In further analysis CNAs among an additional 22 prostate tumor xenografts, we identified four additional HODs at 5q21.1 that affected *CHD1* (Figure 2). One of the HODs in Lu81 removed at least 10 internal exons of *CHD1*.

Analyzing the tumors with *CHD1* HODs, we noticed multiple small size HODs that clustered in the vicinity of particular regions on the same chromosome (Figures 1 and 2). These clustered HODs may be derived from a single event, such as chromothripsis[8], that led to the initial genomic deletions and genomic structural alterations that resulted in additional HODs. This assumption is supported by our initial observation that complete loss of *CHD1* was associated with a large number of HODs at other locations in the tumor genomes in comparison to complete loss of the *PTEN* gene in the JHH cohort. Analyzing the relationship between loss of *CHD1* and additional HODs in the KI cohort from Sweden, we have now confirmed that tumors with complete loss of *CHD1* harbored a significantly larger number of additional HODs (~ 4.64 HODs/genome) than the tumors containing

either complete loss of *PTEN* (~0.53 HODs/genome, P = 0.0001) or no CNAs at *CHD1* and/or *PTEN* (~ 0.3 HODs/genome; $P = 9.95 \times 10^{-8}$).

Table 2. Summary of CHD1 homozygous deletions in patients with PCa from JHH and KI cohorts

Sample ID	chromosome	start	end	cytoband	length(bps)	# markers	Genes
588T	chr5	98,160,688	98,298,394	5q21.1	137,706	65	CHD1
399T	chr5	98,115,300	98,281,597	5q21.1	166,297	78	CHD1,RGMB
85T	chr5	98,105,777	98,273,138	5q21.1	167,361	67	CHD1,RGMB
4847T	chr5	98,139,529	98,433,984	5q21.1	294,455	155	CHD1,RGMB
241T	chr5	98,265,502	98,668,019	5q21.1	367456	68	CHD1
810.T	chr5	98,127,715	98,497,361	5q21.1	369,646	61	CHD1,RGMB
4988T	chr5	98,060,129	98,448,371	5q21.1	388,242	207	CHD1,RGMB
9247T	chr5	98,257,535	98,701,741	5q21.1	444,206	261	CHD1
47T	chr5	98,191,265	98,773,393	5q21.1	582,128	93	CHD1
9158T	chr5	98,016,474	98,686,510	5q21.1	670,036	365	CHD1,RGMB
7214T	chr5	98,088,384	98,829,661	5q21.1	741,277	414	CHD1,RGMB
7421T	chr5	97,388,612	98,302,482	5q21.1	913,870	525	CHD1,RGMB
5605T	chr5	98,231,620	99,198,739	5q21.1	967,119	544	CHD1
4753T	chr5	98,174,141	99,379,726	5q21.1	1,205,585	742	CHD1
172T	chr5	96,850,630	98,257,832	5q15 - 5q21.1	1,407,202	179	CHD1,RGMB
5867T	chr5	97,192,657	98,969,287	5q15 - 5q21.1	1,776,630	990	CHD1,RGMB
4750T	chr5	97,013,621	98,836,222	5q15 - 5q21.1	1,822,601	1057	CHD1,RGMB
460.T	chr5	96,648,385	98,475,618	5q15 - 5q21.1	1,827,233	258	CHD1,RGMB
7067T	chr5	97,754,404	99,936,712	5q21.1	2,182,308	1259	CHD1,FAM174A,RGMB
1009.T	chr5	97,373,780	99,788,692	5q21.1	2,414,912	348	CHD1,RGMB
982.T	chr5	97,849,266	100,746,972	5q21.1	2,897,706	451	CHD1,FAM174A,RGMB,ST8SIA4

Loss of CHD1 is associated with a number of CNAs in other regions of the tumor genome. We next analyzed the distribution of these additional HODs in tumors with complete loss of *CHD1*. In the KI cohort, most of these additional HODs were not randomly distributed, but rather appeared to be preferentially located on chromosomes 2, 4, 5 and 6 with a P-value of 9.91×10^{-10}, 5.12×10^{-13}, $<10^{-16}$, and 0.05, respectively. These results are consistent to what we observed previously in the JHH cohort except for chromosome 4 where no additional HODs was found in the tumors with complete loss of *CHD1*. Some recurrent additional HODs targeted the same region or affected the same genes (Figures 1), while other additional HODs occurred only once in tumors harboring *CHD1* HOD.

To further evaluate the effects of loss of *CHD1* on the changes in CNA signature among the tumor genomes, we first tested the association between any deletion at *CHD1* and the other 19 CNAs using their representative genes identified by GISTIC (Table 3). Deletion of *CHD1* was positively associated with deletions of *LRP1B* at 2q22.1, *PDE4D* at 5q11.2, *MAP3K7* at 6q15 and gain of *COL1A2* at 7q21.3 in both of the cohorts. We next compared the GISTIC signatures with or without the tumors harboring *CHD1* deletions. As shown in the Figure 3, removing the tumors harboring *CHD1* deletions (right panels in A, B, C and D) substantially reduced the significance levels of signature peaks associated with deletions of *LRP1B* at 2q22.1, *PDE4D* at 5q11.2, *MAP3K7* at 6q15 and gain of *COL1A2* at 7q21.3 (marked by light blue ovals), in comparison to the significance levels of these signature peaks derived from all tumors including the ones harbored *CHD1* deletions (left panels in A, B, C and D). These significant concurrences of CNAs suggest a novel collaborative CNA-network among these loci in the evolution of the PCa tumor genome.

In addition, we observed a significantly negative correlation between CNAs at *CHD1* and *TMPRSS2-ERG* on 21q22 (Table 3) in both of the JHH and the Swedish cohorts (P = 0.0057 for the direction of association). Indeed, none of the 21 patients with *CHD1* HOD harbored the deletion from

Table 3. Correlations between loss of *CHD1* and CNAs at other genes (loci)

CNAs	statistics	Loss of CHD1	
		JHH cohort	Swedish cohort
TMPRSS2-ERG	Fisher's Exact Test P-value (2-Tail)	0.02368218	0.012636005
TMPRSS2-ERG	CorrCoef	-0.19473793	-0.240391033
PTEN	Fisher's Exact Test P-value (2-Tail)	0.248201157	0.34159649
PTEN	CorrCoef	-0.113065273	-0.109339848
MAP3K7	Fisher's Exact Test P-value (2-Tail)	2.85E-07	1.50402E-05
MAP3K7	CorrCoef	0.439710571	0.428768016
TP53	Fisher's Exact Test P-value (2-Tail)	0.54102129	0.798303864
TP53	CorrCoef	-0.065212614	-0.050056323
RB1	Fisher's Exact Test P-value (2-Tail)	0.451427643	0.004397239
RB1	CorrCoef	0.068089313	0.290383038
MYC	Fisher's Exact Test P-value (2-Tail)	0.162614144	1
MYC	CorrCoef	0.120854677	0.019728535
BNIP3L	Fisher's Exact Test P-value (2-Tail)	0.444064901	0.482534769
BNIP3L	CorrCoef	-0.067313798	-0.081133646
CDKN1B	Fisher's Exact Test P-value (2-Tail)	0.104997751	0.788994237
CDKN1B	CorrCoef	0.141416117	-0.044206126
RYBP	Fisher's Exact Test P-value (2-Tail)	0.340326948	0.175422177
RYBP	CorrCoef	-0.089596387	-0.151340971
LRP1B	Fisher's Exact Test P-value (2-Tail)	0.000168143	6.71E-07
LRP1B	CorrCoef	0.343794504	0.525592009
ADAR	Fisher's Exact Test P-value (2-Tail)	0.769399639	0.677334081
ADAR	CorrCoef	0.028716905	-0.074141957
DISC1	Fisher's Exact Test P-value (2-Tail)	0.015104857	1
DISC1	CorrCoef	0.222909155	0.014594486
ATP1B3	Fisher's Exact Test P-value (2-Tail)	1	1
ATP1B3	CorrCoef	-0.015521471	-0.00201423
PDE4D	Fisher's Exact Test P-value (2-Tail)	0.001329578	0.006229921
PDE4D	CorrCoef	0.284273975	0.293299855
COL1A2	Fisher's Exact Test P-value (2-Tail)	0.039105473	0.010502274
COL1A2	CorrCoef	0.182162519	0.270840678
TPD52	Fisher's Exact Test P-value (2-Tail)	0.165739199	1
TPD52	CorrCoef	0.124584732	0.006087752
USP10	Fisher's Exact Test P-value (2-Tail)	0.25958319	0.458785599
USP10	CorrCoef	-0.100586846	-0.093881932
SERPINB5	Fisher's Exact Test P-value (2-Tail)	0.649764772	0.781384193
SERPINB5	CorrCoef	-0.060275857	0.035335876
HTR3A	Fisher's Exact Test P-value (2-Tail)	0.043353723	NT
HTR3A	CorrCoef	0.184011165	NT

*NT = not tested because of not significant in GISTIC analysis.

3' of *TMPRSS2* to 5' of *ERG*, which is statistically significant (P = 7.34 X 10^{-4}, Fisher's exact test). These findings indicate that mutually exclusive selection of these two CNAs might occur during proliferation of PCa cells, resulting in two distinct subgroups of PCa.

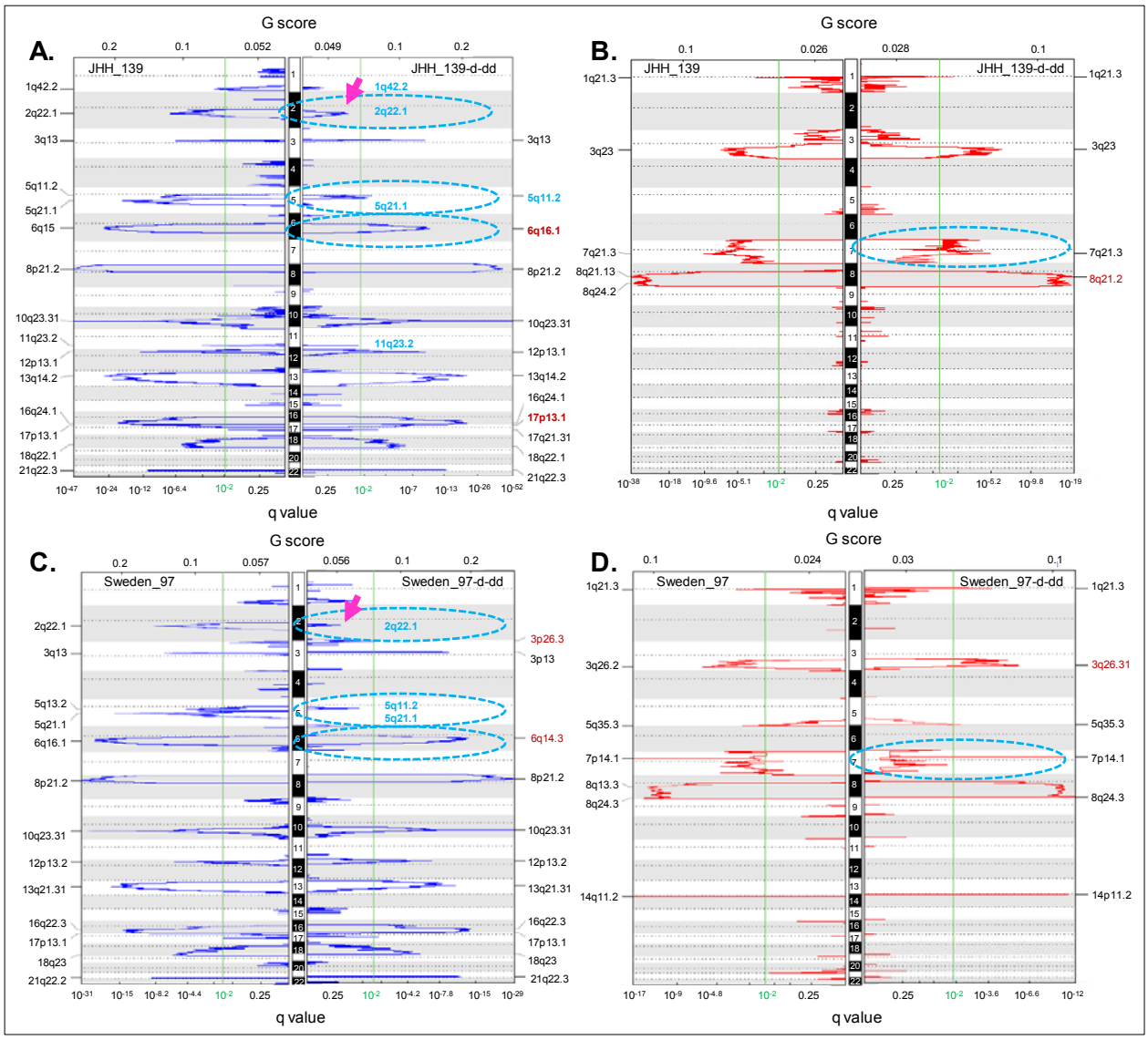

Figure 3. Effects of reducing gene dosage of *CHD1* on the changes in the signatures of deletions (A, C) and amplifications (B, D) among the tumor genomes in the JHH (A, B) and Swedish (C, D) cohorts. Left and right Y axes represent cytoband. Black & white vertical bar in the middle represents chromosome. Green vertical line depicts FDR of 0.01. Top and bottom X axes represent G-score and q-value, respectively. Left panels represent CNAs identified by GISTIC among all tumors including the ones harboring *CHD1* HOD. Right panels represent CNAs identified GISTIC among all tumors excluding the ones harboring *CHD1* HOD. Light blue ovals mark CNAs with substantial changes of the same regions, and cytobands in red represent peak changes, after removing tumors harboring *CHD1* HOD.

Association between CHD1 associated CNAs/genes and clinicopathologic characteristics. To explore the clinical implications of *CHD1* associated genomic structural changes as described above, we performed a correlation analysis between CNAs of *CHD1*, *MAP3K7*, *LRPB1*, *PDE4D*, *COL1A2* or TMPRSS2-ERG and PCa specific death, Gleason score, PSA, tumor stage or biochemical recurrence of PCa. As shown in Table 4, deletions at *CHD1*, *MAP3K7*, *PDE4D and gain of COL1A2* were significantly associated with tumors having a higher Gleason score > 7 in the JHH cohort (P = 0.0329, P = 0.001, P = 0.0102, P = 0.032, respectively). However, the associations of CNAs at these genes with Gleason score were not found in the KI cohort. In addition, none of CNAs at these genes was found to be associated with other clinicopathological parameters, including preoperative PSA, tumor stage, biochemical recurrence and PCa specific death among the patients in these two cohorts. These findings warrant further investigation using additional larger cohorts to illustrate exact clinical implications of *CHD1* associated genomic structure alterations.

Table 4. Association between *CHD1* associated CNAs/genes and clinicopathologic characteristics

JHH Cohort	Death		Gleason		PSA		T-Stage		Recurrence	
Gene	OR(95% CI)	P	OR(95% CI)	P	OR(95% CI)	P	OR(95% CI)	P	OR(95% CI)	P
T_E	1.89(0.73 - 4.88)	0.1869	0.78(0.34 - 1.77)	0.5463	0.72(0.33 - 1.56)	0.4018	0.96(0.43 - 2.17)	0.922	0.36(0.09 - 1.48)	0.1555
MAP3K7	1.24(0.49 - 3.11)	0.6459	3.61(1.68 - 7.77)	0.001	1.53(0.75 - 3.1)	0.2393	1.18(0.56 - 2.49)	0.663	0.46(0.13 - 1.69)	0.2449
CHD1	1.71(0.65 - 4.51)	0.2752	2.38(1.07 - 5.26)	0.0329	0.98(0.45 - 2.11)	0.9563	0.84(0.36 - 1.98)	0.695	1.2(0.25 - 5.71)	0.8188
LRP1B	1.2(0.4 - 3.62)	0.7418	1.03(0.4 - 2.63)	0.953	1.45(0.61 - 3.45)	0.4058	0.78(0.28 - 2.18)	0.632	1.18(0.19 - 7.37)	0.8581
PDE4D	1.91(0.7 - 5.25)	0.21	3.09(1.31 - 7.3)	0.0102	1.54(0.67 - 3.54)	0.3156	2.03(0.84 - 4.9)	0.116	5.16(0.57 - 46.83)	0.145
COL1A2	1.81(0.66 - 4.95)	0.2503	2.55(1.08 - 6.01)	0.032	0.73(0.3 - 1.75)	0.4778	0.65(0.25 - 1.69)	0.376	0.48(0.11 - 2.03)	0.3161

KI Cohort	Death		Gleason		PSA		T-Stage		Recurrence	
Gene	OR(95% CI)	P	OR(95% CI)	P	OR(95% CI)	P	OR(95% CI)	P	OR(95% CI)	P
T_E	1.03(0.1 - 10.46)	0.9787	2.01(0.44 - 9.29)	0.3707	1.51(0.53 - 4.29)	0.4404	1.62(0.37 - 7.17)	0.527	0.78(0.27 - 2.21)	0.6354
MAP3K7	1.46(0.2 - 10.84)	0.713	0.46(0.09 - 2.45)	0.364	0.65(0.25 - 1.69)	0.3728	0.74(0.17 - 3.2)	0.689	1.15(0.49 - 2.71)	0.7536
CHD1	1.1(0.11 - 11.17)	0.9358	1.21(0.22 - 6.57)	0.8266	1.4(0.47 - 4.14)	0.5433	0.4(0.05 - 3.47)	0.409	0.61(0.22 - 1.68)	0.338
LRP1B	1.03(0.1 - 10.46)	0.9787	4.29(0.95 - 19.27)	0.0577	0.73(0.23 - 2.33)	0.5996	0.4(0.05 - 3.47)	0.409	0.71(0.26 - 1.9)	0.490
PDE4D	2.06(0.2 - 21.42)	0.5468	0.82(0.09 - 7.32)	0.8576	1.02(0.28 - 3.75)	0.9741	1.77(0.32 - 9.77)	0.512	1.03(0.3 - 3.49)	0.965
COL1A2		0.9715	0.91(0.1 - 8.24)	0.9363	2.86(0.79 - 10.4)	0.1112	0.88(0.1 - 7.84)	0.905	2.29(0.63 - 8.29)	0.2055

CHD1 associated CNAs/genes in autopsy metastases from subjects who died from PCa. To further investigate the clinical implications of *CHD1* associated CNAs, we analyzed 91 tumor metastases of 30 autopsy patients from JHH using the Affymetrix SNP array 6.0. As shown in

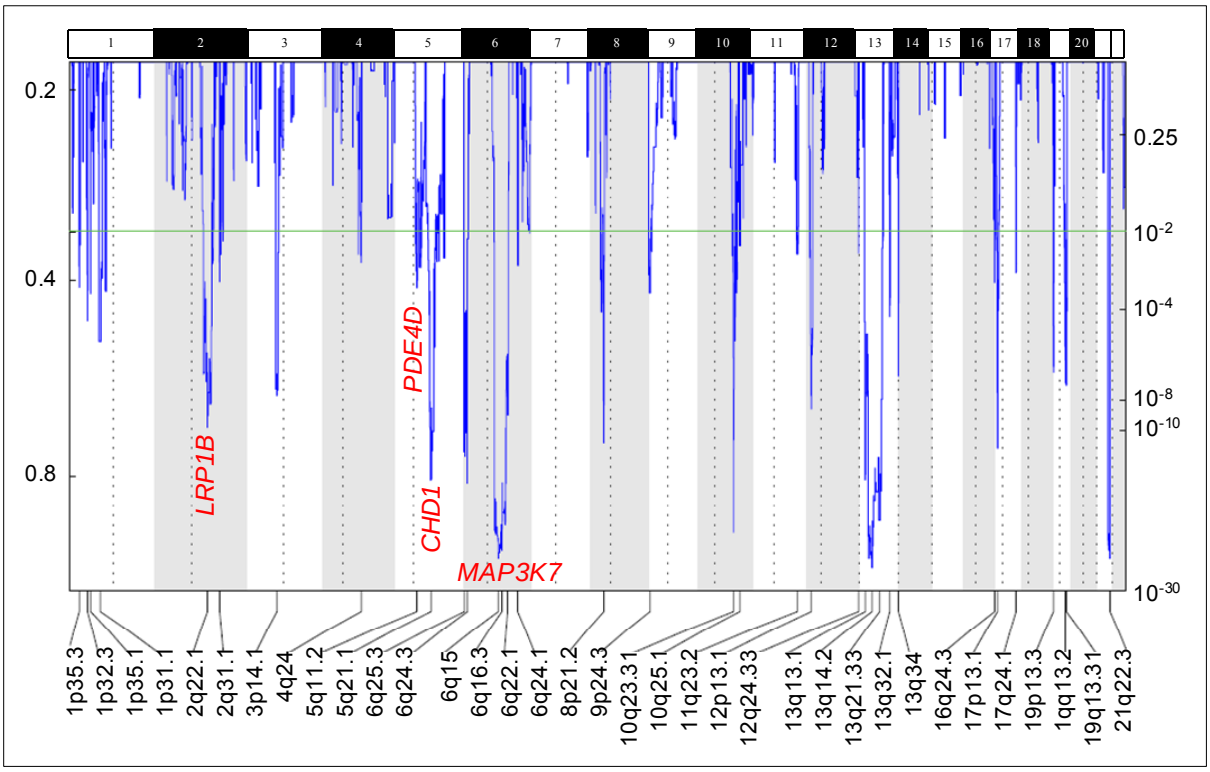

Figure 4. Deletions of *CHD1*, *MAP3K7*, *PDE4D* and *LRP1B* in autopsy metastases from patients who died from PCa. GISTIC was performed using DNA copy number data from 91 tumor metastases to identify significant CNAs in patients who died from PCa. Left and right Y axes represent G-score and q-value, respectively. Black & white horizontal bar on the top represents chromosome. Green horizontal line depicts FDR of 0.01. Bottom X axis represents cytoband.

Figure 4, the signature alterations of genomic structure, including deletions of *CHD1*, *MAP3K7*, *PDE4D* and *LRP1B* identified in clinically localized PCa, were also observed metastases, suggesting that these CNAs might be preserved as cancer cells metastasized to other organs from

the prostate and contribute to death of patients. These results underscore the significance of loss of *CHD1* in PCa progression.

CNAs and morphologic changes after knockdown expression of CHD1. The data presented above suggest that loss of *CHD1* may predispose cells to genomic deletions, potentially at specific loci. To begin to address this question, we chose a well-established human cell transfection model, HEK293, for manipulating *CHD1* expression and analyzed CNAs in cells with stable knockdown of Chd1 protein expression. We identified a deletion that affected *LRP1B* in a cell line stably transfected with *CHD1* shRNA (Figure 4D), which is consistent with our findings in the primary tumors, and suggests a causal relationship. The deletion at *LRP1B* was not observed in the cells either without transfection or stably transfected with control shRNA. We also observed one HOD each on chromosomes 3 and X (Figures 4B and 4C), as well as hemizygous deletions (data not shown) on chromosomes 16 and 18 in the cell lines stably transfected with *CHD1* shRNA but not in these two types of control cells.

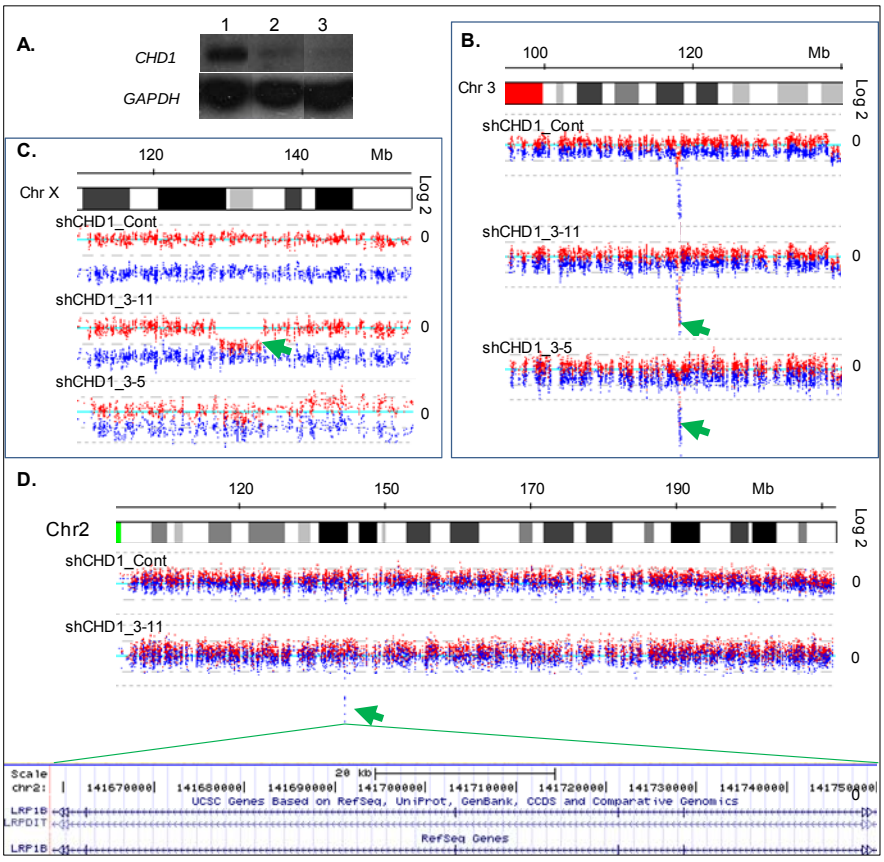

Figure 5. Homozygous deletions (marked by green arrows) identified using allele specific analysis in human HEK293 cells stably transfected by *CHD1* shRNA. DNA from HEK293 cells without transfection was used as a reference for allele specific DNA copy number analysis. Blue and red dot-lines represent different alleles. Light blue horizontal line is the baseline (log2 = 0). Chr, chromosome. A, Western blot showing knockdown of Chd1 protein expression by shRNAs against *CHD1* in a stably transfected HEK293 cell lines shCHD1_3-11(lane 2) and shCHD1_3-5 (lane 3), in comparison to that in cells stably transfected by control shRNAs (shCHD1_Cont, lane 1). D, a hemizygous deletion on chromosome 2q affected the internal exons of *LRP1B* in cells stably transfected with *CHD1* shRNA (shCHD1_3-11), but not in cells stably transfected by control shRNAs (shCHD1_Cont).

To assess possible phenotypic alterations associated with *CHD1* down-regulation, we chose to use our MPECs model because the cells maintain progenitor cell characteristics over long-term culture and reflect the true nature of prostate epithelial stem cells *in vivo*[9]. We infected the MPECs using lentiviruses expressing *CHD1* and control shRNAs. As shown in Figure 6b, *CHD1* shRNA effectively reduced expression of Chd1 protein. In clonogenic analysis we observed that MPECs expressing *CHD1* shRNA formed more colonies than the cells expressing control shRNA (Figure 6a). Quantitative analysis of the clonogenic data revealed that cells with knockdown expression of *CHD1* displayed a consistently higher (P = 0.0489) survival and proliferation rate (Figure 6b). This result suggests that silencing endogenous *CHD1* expression might enhance cell clonogenicity or survivability. We further analyzed the morphological characteristics of MPECs growth, using silenced expression of endogenous *CHD1* in a three-dimensional (3D) culture system. As expected, cell spheroids were formed by MPECs transfected with control shRNA (Figure 6c). Surprisingly, the MPECs transfected with *CHD1* shRNA formed branch structures growing into the

collagen matrix, with significantly ($P < 0.0001$) lengthening of branches and side branches (Figures 6d, 6e) which were not observed in cells transfected with control shRNA. These characteristics suggest that silenced *CHD1* expression could significantly enhance cell invasiveness and/or developmental changes.

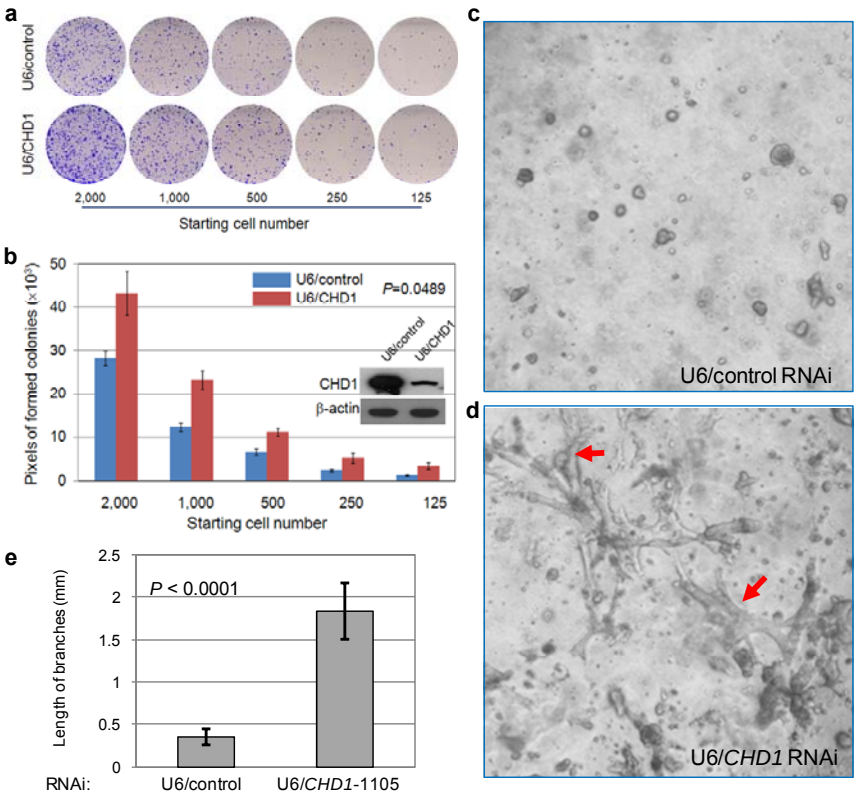

Figure 6. Down-regulation of Chd1 in mouse prostate epithelial cells (MPECs) alters morphological characteristics in the growth of the cells. (**a**) Clonogenic assay shows more colonies formed from the cells with reduced level of Chd1 protein (U6/CHD1). (**b**) Quantitative data of clonogenic assay demonstrate that cells with knockdown expression of Chd1 displayed a larger number of pixels from formed colonies. Western blotting shows a reduction of Chd1 protein in MPECs transfected by *CHD1* shRNA (U6/*CHD1*) in comparison to those transfected by control shRNA (U6/control). (**c**) Cell spheroids formed by MPECs transfected with control shRNA in a three-dimensional culture system. (**d**) Multiple branching structures (marked by red arrows) were generated by MPECs transfected with *CHD1* shRNA in a three-dimensional culture system. (**e**) Comparison of the length of branches formed by the cells transfected with U6/control or U6/*CHD1* shRNA. Four representative views from each of the treatments were taken and five of the longest branches within each of the views were measured. The average and standard deviation are presented. Significantly longer branches formed by the cells transfected with U6/*CHD1* shRNA in this three-dimensional culture indicate an invasive property of cells with down-regulated Chd1. All of the experiments were carried out in triplicates.

Developing cell lines with stable knockdown expression of CHD1/ MAP3K7 from prostate epithelial and PCa cells. To further investigate the biological role of *CHD1* in the development and

Table 5. Examples of developing stable cell lines with knockdown expression of *CHD1*

Summary	Western Blot_a		Western Blot_b		Western Blot_c	
Name of cell line/shRNA	a	P/N/R*	b	P/N/R	c	P/N/R
iRWPE-CHD-1	10/4/2012	N	1/9/2013	N	4/8/2013	N
iRWPE-CHD-6	10/4/2012	N	1/9/2013	N	4/8/2013	N
iRWPE-CHD-7	10/2/2012	N	1/9/2013	N	4/8/2013	R
iRWPE-CHD-8	10/2/2012	R				
iRWPE-CHD-9	10/2/2012	N	1/9/2013	N	4/8/2013	N
iRWPE-CHD-10	10/2/2012	P				
iRWPE-CHD-11	10/2/2012	P				
iRWPE-CHD-12	10/2/2012	N	1/9/2013	N	4/8/2013	R
iRWPE-CHD-13	10/2/2012	N	1/9/2013	N/R		
iRWPE-CHD-14	10/2/2012	N	1/9/2013	N	4/8/2013	P
iRWPE-CHD-15	10/2/2012	R				
iRWPE-CHD-16	10/2/2012	P				
iRWPE-CHD-17	12/3/2012	N	1/9/2013	N	4/8/2013	N

*P/N/R: Positive/Negative/Reduced, only negative cell lines were used in subsequent experiments.

progression of PCa, we designed two new shRNAs against *MAP3K7* and cloned effective shRNAs against *CHD1* and *MAP3K7* into new vectors for transduction into various cell lines as we proposed in the grant application. During selection of different clones, with each derived from a single cell initially infected with the lentivirus expressing these shRNAs, we noticed that inhibition of Chd1 expression in some cell lines was not stable even after more than 5 months of selection (Table 5). Therefore, only the ones with stable inhibition of the target genes after 3 western-blot confirmations were selected for subsequent experiments. We have currently developed 25 cell lines with stable knockdown expression of *CHD1* from normal prostate epithelial cells and 20 cell lines with 2 western-blot confirmations from PC-3 cancer cells. In addition, we also obtained 2 cell lines with knockdown expression of *MAP3K7* or *CHD1* with each from MPECs, and one cell line with knockdown expression of *MAP3K7* or *CHD1* with each from DU145 and LNCaP prostate cancer cells. These newly generated cell lines will be used to assess the biological role of *CHD1* in the development of PCa in years 2 and 3.

Discussion

Using an unbiased genome-wide analysis of tumor DNA from multiple cohorts, we have uncovered and validated a chromatin remodeler encoded by *CHD1* as one of the two most frequent homozygously deleted genes in the tumor genome of PCa. Recent studies on the exome and the whole-genome of clinically localized[10, 11] and castration-resistant[12] PCa have further confirmed our initial findings. Importantly, we have identified novel *CHD1*-associated collaborative CNAs which may shed light on the development and progression of PCa.

Among the three genes concurrently deleted with *CHD1*, *LRP1B* and *PDE4D* are apparently located at fragile sites on chromosomes of 2 and 5, respectively[13]. However, *MAP3K7* seems not associated with inherent fragility and rather may function as a tumor suppressor gene. Encoding TGF-β activated kinase-1 (Tak1), *MAP3K7* has been reported to be frequently deleted in PCa, the occurrence of which is highly associated with high grade disease[14]. Recent work has demonstrated a tumor suppressive role of *MAP3K7* in liver cancer[15] and PCa[16]. Therefore, it will be important to uncover how *CHD1* and *MAP3K7* interact to affect PCa development.

Together with preliminary results from HEK293 cells stably transfected with *CHD1* shRNA, these data indicate that *CHD1* may either play a role in protecting the genome from loss of DNA, or it may, in conjunction with the other associated CNAs, provide selection and/or growth advantages for tumor cells during the development of PCa. It is plausible that the chromatin remodeler encoded by *CHD1* may indirectly protect DNA because it facilitates deposition of H3 histone into chromatin[17, 18]. In addition, direct binding of *CHD1* to DNA[19] may provide an alternative mechanism of protection while it is unknown whether *CHD1* is directly involved in DNA repair. Furthermore, post-translational modifications to histones have been reported to influence DNA repair[20]. Various cell lines with stable knockdown expression of target genes described above will provide better biological systems to further investigate the role of *CHD1* in DNA repair and genome instability in years 2 and 3 as we proposed.

KEY RESEARCH ACCOMPLISHMENTS

1) Collected and updated new tumor/normal samples and clinical information of PCa patients.
2) Performed DNA copy number analysis, identified significant CNAs, and assessed the correlations between *CHD1* associated CNAs/genes and clinicopathologic characteristics in multiple cohorts.
3) Developed cell lines with knockdown expression of target genes and explored preliminary effects of *CHD1* knockdown in pilot experiments.

REPORTABLE OUTCOMES

1) Homozygously deleted genes in the tumor genome of PCa (Tables 1 and 2, Figures 1, 2 and 4).
2) Correlations between loss of *CHD1* and CNAs at other genes (loci (Table 3 and Figure 3).
3) Associations between *CHD1* associated CNAs/genes and clinicopathologic characteristics (Table 4).
4) Preliminary *in vitro* effects of *CHD1* knockdown (Figures 5 and 6).
5) New cell lines with knockdown expression of *CHD1*/*MAP3K7* (Table 5).

CONCLUSION

1) We have made a huge progress in achieving the goals as described in the approved statement of work.
2) We have identified and validated that 1) *CHD1* is second only to *PTEN* as the most frequent homozygously deleted gene in PCa, and 2) tumors with loss of *CHD1* represent a unique and distinct subtype of PCa.

REFERENCES

1. Sui G, Shi Y. Gene silencing by a DNA vector-based RNAi technology. Methods Mol Biol 2005;309: 205-218.
2. Sui G, Soohoo C, Affar el B, Gay F, Shi Y, Forrester WC. A DNA vector-based RNAi technology to suppress gene expression in mammalian cells. Proc Natl Acad Sci U S A 2002;99(8): 5515-5520.
3. Deng Z, Wan M, Cao P, Rao A, Cramer SD, Sui G. Yin Yang 1 regulates the transcriptional activity of androgen receptor. Oncogene 2009;28(42): 3746-3757.
4. Deng Z, Wan M, Sui G. PIASy-mediated sumoylation of Yin Yang 1 depends on their interaction but not the RING finger. Mol Cell Biol 2007;27(10): 3780-3792.
5. Barclay WW, Cramer SD. Culture of mouse prostatic epithelial cells from genetically engineered mice. Prostate 2005;63(3): 291-298.
6. Cao P, Deng Z, Wan M, Huang W, Cramer SD, Xu J, Lei M, Sui G. MicroRNA-101 negatively regulates Ezh2 and its expression is modulated by androgen receptor and HIF-1alpha/HIF-1beta. Mol Cancer 2010;9: 108.
7. Beroukhim R, Getz G, Nghiemphu L, Barretina J, Hsueh T, Linhart D, Vivanco I, Lee JC, Huang JH, Alexander S, Du J, Kau T, Thomas RK, Shah K, Soto H, Perner S, Prensner J, Debiasi RM, Demichelis F, Hatton C, Rubin MA, Garraway LA, Nelson SF, Liau L, Mischel PS, Cloughesy TF, Meyerson M, Golub TA, Lander ES, Mellinghoff IK, Sellers WR. Assessing the significance of chromosomal aberrations in cancer: methodology and application to glioma. Proc Natl Acad Sci U S A 2007;104(50): 20007-20012.
8. Stephens PJ, Greenman CD, Fu B, Yang F, Bignell GR, Mudie LJ, Pleasance ED, Lau KW, Beare D, Stebbings LA, McLaren S, Lin ML, McBride DJ, Varela I, Nik-Zainal S, Leroy C, Jia M, Menzies A, Butler AP, Teague JW, Quail MA, Burton J, Swerdlow H, Carter NP, Morsberger LA, Iacobuzio-Donahue C, Follows GA, Green AR, Flanagan AM, Stratton MR, Futreal PA, Campbell PJ. Massive genomic rearrangement acquired in a single catastrophic event during cancer development. Cell 2011;144(1): 27-40.
9. Barclay WW, Axanova LS, Chen W, Romero L, Maund SL, Soker S, Lees CJ, Cramer SD. Characterization of adult prostatic progenitor/stem cells exhibiting self-renewal and multilineage differentiation. Stem Cells 2008;26(3): 600-610.
10. Baca SC, Prandi D, Lawrence MS, Mosquera JM, Romanel A, Drier Y, Park K, Kitabayashi N, Macdonald TY, Ghandi M, Van Allen E, Kryukov GV, Sboner A, Theurillat JP, Soong TD, Nickerson E, Auclair D, Tewari A, Beltran H, Onofrio RC, Boysen G, Guiducci C, Barbieri CE, Cibulskis K, Sivachenko A, Carter SL, Saksena G, Voet D, Ramos AH, Winckler W, Cipicchio M, Ardlie K, Kantoff

PW, Berger MF, Gabriel SB, Golub TR, Meyerson M, Lander ES, Elemento O, Getz G, Demichelis F, Rubin MA, Garraway LA. Punctuated evolution of prostate cancer genomes. Cell 2013;153(3): 666-677.
11. Barbieri CE, Baca SC, Lawrence MS, Demichelis F, Blattner M, Theurillat JP, White TA, Stojanov P, Van Allen E, Stransky N, Nickerson E, Chae SS, Boysen G, Auclair D, Onofrio RC, Park K, Kitabayashi N, Macdonald TY, Sheikh K, Vuong T, Guiducci C, Cibulskis K, Sivachenko A, Carter SL, Saksena G, Voet D, Hussain WM, Ramos AH, Winckler W, Redman MC, Ardlie K, Tewari AK, Mosquera JM, Rupp N, Wild PJ, Moch H, Morrissey C, Nelson PS, Kantoff PW, Gabriel SB, Golub TR, Meyerson M, Lander ES, Getz G, Rubin MA, Garraway LA. Exome sequencing identifies recurrent SPOP, FOXA1 and MED12 mutations in prostate cancer. Nat Genet 2012;44(6): 685-689.
12. Grasso CS, Wu YM, Robinson DR, Cao X, Dhanasekaran SM, Khan AP, Quist MJ, Jing X, Lonigro RJ, Brenner JC, Asangani IA, Ateeq B, Chun SY, Siddiqui J, Sam L, Anstett M, Mehra R, Prensner JR, Palanisamy N, Ryslik GA, Vandin F, Raphael BJ, Kunju LP, Rhodes DR, Pienta KJ, Chinnaiyan AM, Tomlins SA. The mutational landscape of lethal castration-resistant prostate cancer. Nature 2012;487(7406): 239-243.
13. Bignell GR, Greenman CD, Davies H, Butler AP, Edkins S, Andrews JM, Buck G, Chen L, Beare D, Latimer C, Widaa S, Hinton J, Fahey C, Fu B, Swamy S, Dalgliesh GL, Teh BT, Deloukas P, Yang F, Campbell PJ, Futreal PA, Stratton MR. Signatures of mutation and selection in the cancer genome. Nature 2010;463(7283): 893-898.
14. Liu W, Chang BL, Cramer S, Koty PP, Li T, Sun J, Turner AR, Von Kap-Herr C, Bobby P, Rao J, Zheng SL, Isaacs WB, Xu J. Deletion of a small consensus region at 6q15, including the MAP3K7 gene, is significantly associated with high-grade prostate cancers. Clin Cancer Res 2007;13(17): 5028-5033.
15. Bettermann K, Vucur M, Haybaeck J, Koppe C, Janssen J, Heymann F, Weber A, Weiskirchen R, Liedtke C, Gassler N, Muller M, de Vos R, Wolf MJ, Boege Y, Seleznik GM, Zeller N, Erny D, Fuchs T, Zoller S, Cairo S, Buendia MA, Prinz M, Akira S, Tacke F, Heikenwalder M, Trautwein C, Luedde T. TAK1 suppresses a NEMO-dependent but NF-kappaB-independent pathway to liver cancer. Cancer Cell 2010;17(5): 481-496.
16. Wu M, Shi L, Cimic A, Romero L, Sui G, Lees CJ, Cline JM, Seals DF, Sirintrapun JS, McCoy TP, Liu W, Kim JW, Hawkins GA, Peehl DM, Xu J, Cramer SD. Suppression of Tak1 promotes prostate tumorigenesis. Cancer Res 2012;72(11): 2833-2843.
17. Konev AY, Tribus M, Park SY, Podhraski V, Lim CY, Emelyanov AV, Vershilova E, Pirrotta V, Kadonaga JT, Lusser A, Fyodorov DV. CHD1 motor protein is required for deposition of histone variant H3.3 into chromatin in vivo. Science 2007;317(5841): 1087-1090.
18. Sims RJ, 3rd, Reinberg D. Stem cells: Escaping fates with open states. Nature 2009;460(7257): 802-803.
19. Stokes DG, Perry RP. DNA-binding and chromatin localization properties of CHD1. Mol Cell Biol 1995;15(5): 2745-2753.
20. Avvakumov N, Nourani A, Cote J. Histone chaperones: modulators of chromatin marks. Mol Cell 2011;41(5): 502-514.